

Negative nonlinear absorption in Er 3+ -doped fluoroindate glass

W. Lozano B., Cid B. de Araújo, L. H. Acioli, and Y. Messaddeq

Citation: *Journal of Applied Physics* **84**, 2263 (1998); doi: 10.1063/1.368292

View online: <http://dx.doi.org/10.1063/1.368292>

View Table of Contents: <http://scitation.aip.org/content/aip/journal/jap/84/4?ver=pdfcov>

Published by the [AIP Publishing](#)



Re-register for Table of Content Alerts

Create a profile.



Sign up today!



Negative nonlinear absorption in Er³⁺-doped fluoroindate glass

W. Lozano B., Cid B. de Araújo, and L. H. Acioli

Departamento de Física, Universidade Federal de Pernambuco, 50670-901 Recife, PE Brazil

Y. Messaddeq

Instituto de Química, UNESP, 14800-900 Araraquara, SP Brazil

(Received 18 July 1997; accepted for publication 15 May 1998)

We report the observation of negative nonlinear absorption in fluoroindate glasses doped with erbium ions. The pumping wavelength is 800 nm which is doubly resonant with Er³⁺ ions transitions. A large nonlinear intensity dependence of the optical transmittance and strong upconverted fluorescence are obtained. The dependence of the upconverted fluorescence intensity with the laser power is described by a system of coupled-rate equations for the energy levels' populations. © 1998 American Institute of Physics. [S0021-8979(98)07816-5]

I. INTRODUCTION

Presently there is great interest in the study of the nonlinear absorption behavior of new materials because of possible photonic applications such as frequency upconversion lasers,^{1,2} all-optical switches,^{3,4} and bistable devices.⁵

Among the new materials available to date, fluoroindate glasses doped with rare earth (RE) ions appear as promising candidates to be used in photonic devices because of the low multiphonon emission rates and high fluorescence efficiencies for RE ions, as compared when they are doping other glasses.

Various spectroscopic studies of RE doped InF₃-based glasses have appeared in recent years. For instance, basic studies on the optical properties of fluoroindate glasses doped with Eu³⁺, Gd³⁺, Pr³⁺, Nd³⁺, Tm³⁺, and Dy³⁺ were reported.^{6–11} Frequency upconversion and energy transfer processes involving Pr³⁺-, Er³⁺-, and Nd³⁺-doped fluoroindate glasses were also presented^{12–16} illustrating the large potentiality of this glass family as efficient optical upconverters. Moreover, applications such as flashlamp pumped lasers,¹⁷ temperature sensor,¹⁸ and processing of waveguides for integrated optics¹⁹ are already known.

In this paper we report the first observation of negative nonlinear absorption (NNA) in Er³⁺-doped fluoroindate glass, at room temperature. This effect, previously observed in highly doped erbium–yttrium aluminum garnets²⁰ and in semiconductors,²¹ is characterized by a decrease of the transmission with increasing intensity. It is usually due to a double resonance of the incident radiation with a pair of electronic transitions. It can be studied directly by observing the transmission through the sample or indirectly by measuring the resulting upconverted radiation as a function of the intensity of the incident laser. This upconverted radiation is only present when the highest excited state has a large radiative branching ratio to the lowest lying states, as is the case presented here. From the applied point of view this effect is also important for optical limiting applications²² and for operation of bistable devices.²³

II. EXPERIMENT

The samples used, prepared according to the procedure described in Refs. 6, 7, 12, and 14 have the following compositions in mol %: (39–*x*) InF₃–20ZnF₂–20SrF₂–16BaF₂–2GdF₃–2NaF–1GaF₃–*x*ErF₃ (*x*=1 and 3). The samples present good optical quality and do not show any crystallization under examination with the optical microscope.

Optical absorption spectra in the 200–800 nm were obtained with a diode array spectrophotometer and the results are similar to the ones already presented in Ref. 14.

The excitation of NNA was performed using a commercial continuous-wave diode laser operating at 800 nm and delivering ~5 mW. The laser beam was focused on the sample using a lens with 10 cm of focal length. The fluorescence, collected perpendicularly to the direction of the incident beam and dispersed by a 0.5 m grating spectrometer, was detected with a GaAs photomultiplier. For the transmittance measurements Si photodiodes were used. The signals were processed with a lock-in or a digital oscilloscope coupled to a personal computer for data processing.

III. RESULTS AND DISCUSSION

Figure 1 shows the dependence of the transmitted beam intensity as a function of the incident laser intensity. The laser wavelength was chosen at 800 nm in order to be simultaneously resonant with one erbium transition originating from the ground state, ⁴I_{15/2}→⁴I_{9/2}, and also with transitions associated to excited states ⁴I_{11/2}→(⁴F_{5/2}, ⁴F_{3/2}) and ⁴I_{13/2}→²H_{11/2}.

The experiments were performed with the two Er³⁺ concentrations available and both samples exhibit NNA which causes a decreasing transmission as the laser intensity is increasing. The obtained results are shown in Fig. 1, where the points represent the experimental data. The solid lines in Fig. 1 were obtained using the expression $T = (1 - R)^2 e^{-\alpha_0 d} [1 + \alpha_2 / \alpha_0 I_0 (1 - R)(1 - e^{-\alpha_0 d})]^{-i}$ for the transmittance, where $R = 0.04$ is the air–glass interface reflectivity, I_0 is the laser intensity on the front surface of the sample, d represents the sample length, α_0 is the measured linear absorption coefficient.

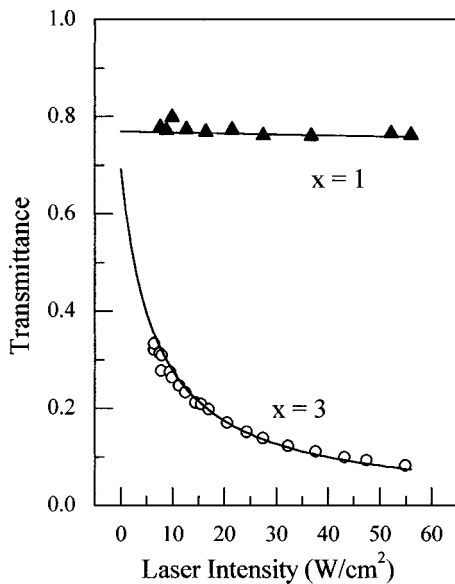


FIG. 1. Transmittance at 800 nm as a function of the incident laser power for the samples with $x=1$ and $x=3$.

cient, and α_2 is the nonlinear absorption coefficient. The parameters used in these fittings are presented in Table I.

The fluorescence spectrum observed in the 500–700 nm range for the sample with $x=3$ is shown in Fig. 2. The spectral bands correspond to transitions ${}^2H_{11/2} \rightarrow {}^4I_{15/2}$ (~520 nm), ${}^4S_{3/2} \rightarrow {}^4I_{15/2}$ (~550 nm), and ${}^4F_{9/2} \rightarrow {}^4I_{15/2}$ (~670 nm). The spectrum for the other sample is similar except for the band intensities which decreases with the erbium concentration.

The frequency upconversion process was monitored through the fluorescence at ~550 nm and the dependence of the emitted signal with the laser intensity is shown in Fig. 3. We note that the sample with $x=3$ presents a strong nonlinear dependence (slope 5 in the log–log plot) while an almost quadratic dependence is observed for the other sample.

We have also studied the dynamics of the frequency upconversion process as a function of the pump intensity. In these temporal studies the excitation beam was chopped at a frequency of 8 Hz while the upconverted fluorescence was monitored with a digital oscilloscope. The temporal resolution of the detection system is 0.1 ms.

Figure 4 shows the dependence of the fluorescence from the $x=3$ sample for four different intensities. It is important to note that the signal rise time is ~10 ms, although the lifetime of the fluorescing level is $0.6 \mu\text{s}$.¹⁴ This behavior indicates that long-lived states participate as intermediate stages in the upconversion process.

In order to understand the upconversion dynamics we first consider the energy level scheme of Fig. 5(a) which

TABLE I. Parameters used to fit the theoretical expression of the intensity dependent transmittance.

	$d(\text{cm})$	$\alpha_0(\text{cm}^{-1})$	$\alpha_2(\text{cm}^{-1}/\text{W})$
$x=1$	0.29	0.317	0.001
$x=3$	0.28	1.028	0.631

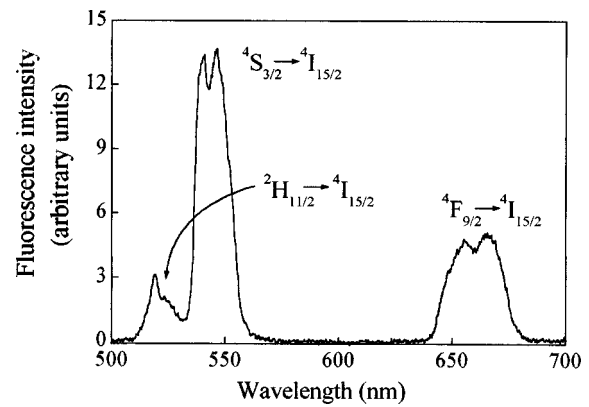


FIG. 2. Upconverted fluorescence spectrum excited with a diode laser operating at 800 nm.

indicates possible steps in the excitation process. The first step is a resonant transition ${}^4I_{15/2} \rightarrow {}^4I_{9/2}$ followed by a fast nonradiative relaxation to level ${}^4I_{11/2}$ followed by a slow nonradiative decay to level ${}^4I_{13/2}$. Excited state absorptions (ESA) to highly excited states, ${}^4I_{11/2} \rightarrow ({}^4F_{3/2}, {}^4F_{5/2})$, and ${}^4I_{13/2} \rightarrow {}^2H_{11/2}$ occur and originate the frequency upconversion emissions.

It is important to note that cross relaxations (${}^2H_{11/2}, {}^4I_{15/2} \rightarrow ({}^4I_{9/2}, {}^4I_{13/2})$ and (${}^4F_{7/2}, {}^4I_{15/2} \rightarrow ({}^4I_{11/2}, {}^4I_{13/2})$) may contribute to increase the population of levels ${}^4I_{11/2}$ and ${}^4I_{13/2}$ and thus the emission at ~550 nm is enhanced. The red emission at ~670 nm (${}^4F_{9/2} \rightarrow {}^4I_{15/2}$) occurs after nonradiative relaxation ${}^4S_{3/2} \rightarrow {}^4F_{9/2}$.

In Fig. 5 we present a simplified scheme for the energy levels including all the essential excitation steps. Level 1 corresponds to the ground state ${}^4I_{15/2}$, level 2 corresponds to either ${}^4I_{11/2}$ or ${}^4I_{13/2}$, and level 3 represents levels ${}^4S_{3/2}$ and all other levels of higher energies. State ${}^4F_{9/2}$ is not considered in the model because the red emission is weaker than the green fluorescence. A four level system was also employed but no significant improvements compared to the

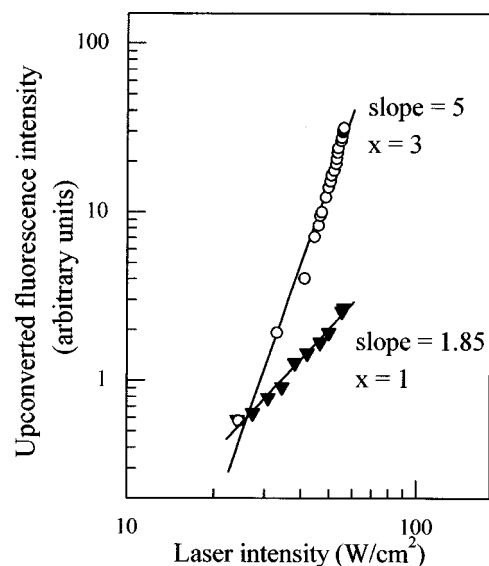


FIG. 3. Dependence of the upconverted fluorescence emitted at 550 nm as a function of the incident laser intensity.

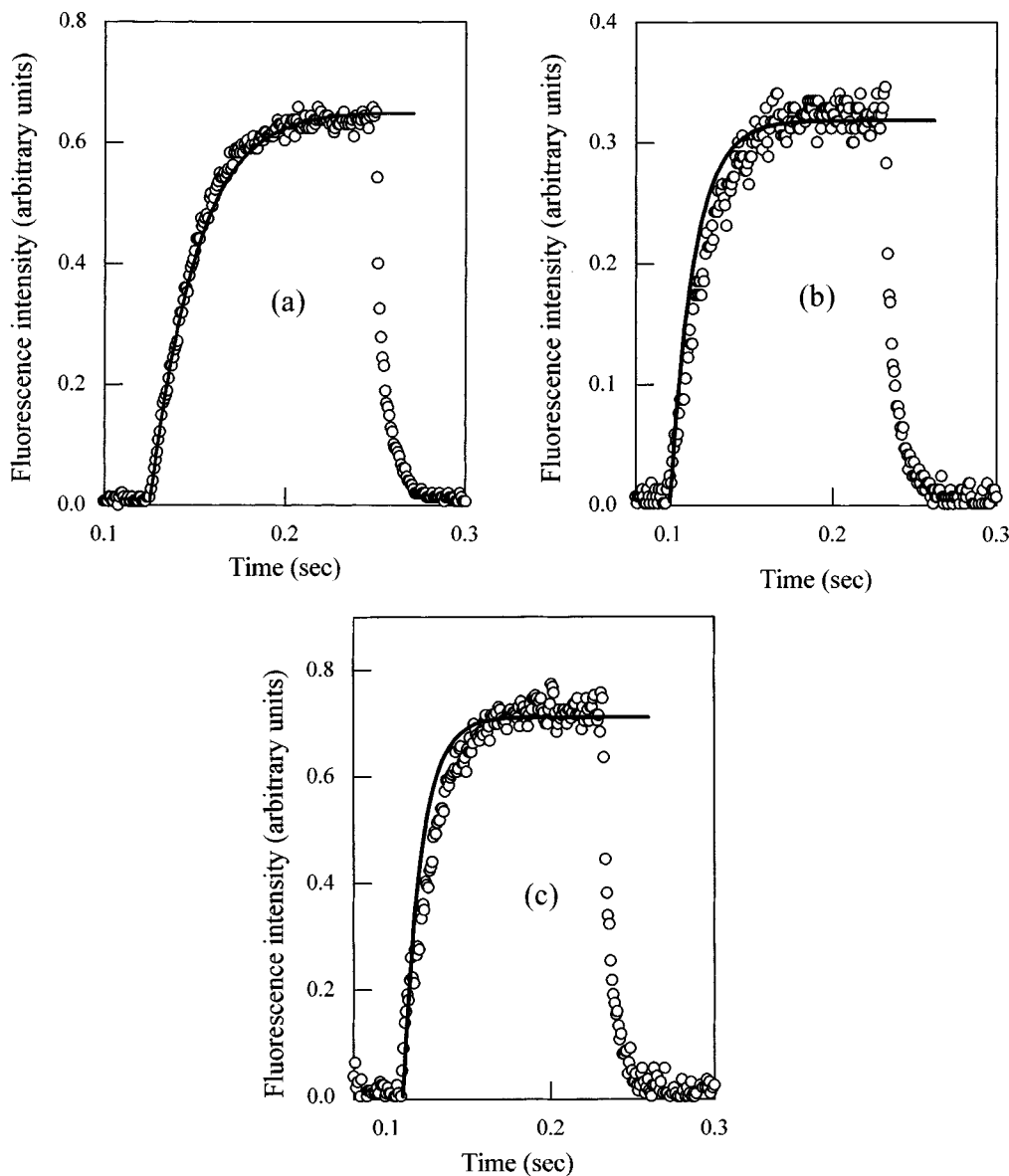


FIG. 4. Fluorescence intensity at 550 nm vs time during laser illumination with an excitation intensity of 56.6 W/cm² (a); 24 W/cm² (b); and 7.5 W/cm² (c). Sample with $x=3$.

three level model are obtained. The observed temporal behavior is reproduced using a rate-equation approach which takes into account the contributions due to the two pumping rates $R_1(1 \rightarrow 2)$ and $R_2(2 \rightarrow 3)$. The equations for the population densities assume the form:

$$\dot{n}_1 = -R_1 n_1 + W_2 n_2 + W_{31} n_3 - S n_1 n_3, \tag{1}$$

$$\dot{n}_2 = R_1 n_1 - (R_2 + W_2) n_2 + W_{32} n_3 + 2S n_1 n_3, \tag{2}$$

$$\dot{n}_3 = R_2 n_2 - W_3 n_3 - S n_1 n_3, \tag{3}$$

where n_1 , n_2 , and n_3 denote the population densities in levels 1, 2, and 3, respectively, and $n_1 + n_2 + n_3 = 1$. The parameters W_2 and $W_{31} + W_{32} = W_3$ are the relaxation rates of levels 2 and 3, respectively. S is the effective cross-relaxation parameter associated to processes $[^4S_{3/2}(^2H_{11/2}) \rightarrow ^4I_{9/2}] + [^4I_{15/2} \rightarrow ^4I_{13/2}]$ and $[^4S_{3/2}(^2H_{11/2}) \rightarrow ^4I_{13/2}]$

$+ [^4I_{15/2} + ^4I_{9/2}]$. The software package MATHEMATICA was used to solve numerically the system of equations presented above.

The agreement of the model with the experimental results can be verified in Fig. 4, where the solid line was obtained using the parameters indicated in Table II. The values of W_{31} , W_{32} , and W_2 were obtained from Refs. 14 and 16. The ratio between the pumping rates R_1 and R_2 , and the cross-relaxation rate S , were determined from the upconversion intensity measurements as a function of the incident laser intensity. From the steady state solution of Eqs. (1)–(3) we can calculate the upconverted fluorescence and compare the results with the observed behavior under cw excitation. In Fig. 6 we show the results of the comparison with the experimental results from Fig. 3. It is important to mention that the parameters used here are the same as obtained from the fitting of the transient experiments.

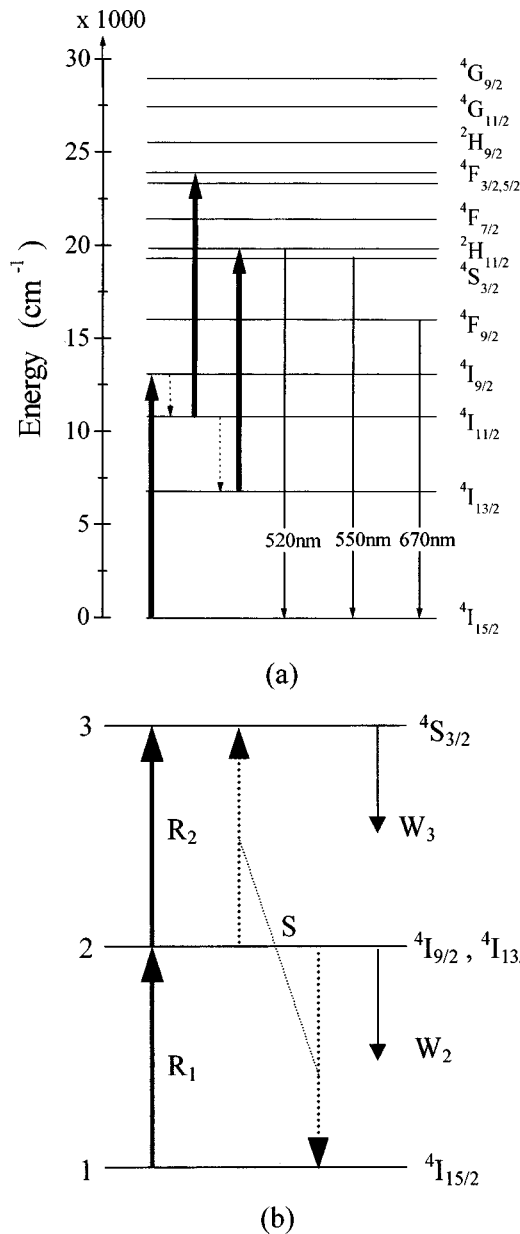


FIG. 5. Simplified energy levels scheme. (a) Relevant levels of Er^{3+} ; and (b) three-level model used in the calculations.

We note that the dependence of the cross-relaxation rate with the erbium concentration (as shown in Table II) is a consequence of the change in the distances between the active ions. This dependence explains why the NNA effect is less pronounced in the sample with $x=1$. The nonlinear behavior of transmittance and upconverted fluorescence as a function of laser intensity is mainly due to the large cross-

TABLE II. Parameters used to fit the temporal behavior of the upconverted fluorescence.

	$W_{31}(\text{s}^{-1})$	$W_{32}(\text{s}^{-1})$	$W_2(\text{s}^{-1})$	$S(\text{s}^{-1})$	R_1/R_2
$x=1$	638	262	100	1750	0.012
$x=3$	781	321	109	1300	0.012

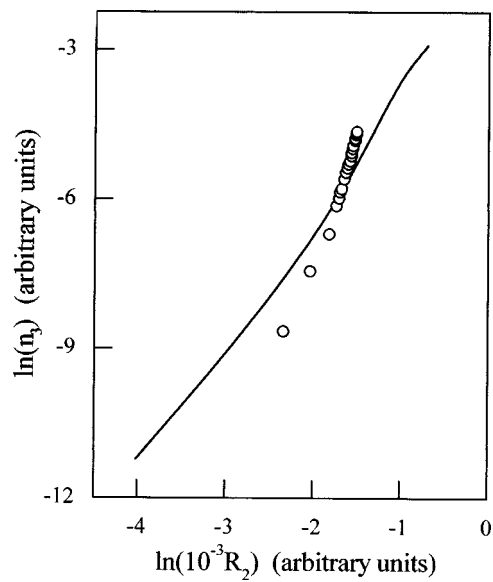


FIG. 6. Upconverted fluorescence intensity vs the pumping rate (R_2). The circles are experimental results and the solid line was obtained using the rate equation approach to calculate the population of the fluorescing level. The values for the parameters are those indicated in Table II obtained fitting the theoretical expressions to the results of Fig. 4.

relaxation which enables the excitation of two ions in the ($^4I_{11/2}, ^2I_{13/2}$) states when pumping transition $^4I_{15/2} \rightarrow ^4I_{9/2}$.

A closely related effect which is also possible to observe with our samples is the phenomenon of photon avalanche.^{16,24-26} The main difference is that in the avalanche effect the sample's absorption is initially very small and constant, with the laser tuned far from resonance in the first step. Under these conditions there is an intensity threshold where the transmission starts to change, which is not what happens in the present measurements. We can say that the negative nonlinear absorption observed for the experimental situation discussed here is a limiting case where the avalanche effect is absent (even for very low powers the transmission depends nonlinearly on the intensity), because the ratio between the pumping ratios, R_1/R_2 , is too large.

V. CONCLUSION

We have reported negative nonlinear absorption in an Er^{3+} -doped fluoroindate glass pumped at 800 nm. The experimental results, obtained using a low power diode laser, depend on the erbium concentration because the interaction among ion pairs which contribute significantly to the NNA process is strongly dependent on the relative distance among Er^{3+} ions. The presented theoretical model agrees with the experimental results and provides an estimate for the effective cross-relaxation rate among erbium ions.

From the results presented here and due to the similarities between fluoroindate glass and fluorozirconate glass, we conclude that other nonlinear effects, such as photon avalanche, may also be observed in InF_3 -based glasses using inexpensive diode lasers with appropriate wavelengths. Further experiments along this line will be performed in the near future.

ACKNOWLEDGMENTS

This work was supported by the Brazilian Agencies Conselho Nacional de Desenvolvimento Científico e Tecnológico (CNPq), Financiadora Nacional de Estudos e Projetos (FINEP), Fundação Coordenação de Pessoal de Nível Superior (CAPES), and Fundação de Amparo à Ciência e Tecnologia (FACEPE). Stimulating discussions with G. S. Maciel and N. Rakov are also acknowledged.

- ¹T. Herbert, R. Wannermacher, R. M. Macfarlane, and W. Length, *Appl. Phys. Lett.* **60**, 2592 (1992).
- ²S. C. Goh, R. Pattie, C. Byrne, and D. Coulson, *Appl. Phys. Lett.* **67**, 768 (1995).
- ³F. Z. Henari, K. H. Cazzini, D. N. Weldon, and W. J. Blaw, *Appl. Phys. Lett.* **68**, 619 (1996).
- ⁴C. B. de Araújo, A. S. L. Gomes, and R. Srivastava, *Appl. Phys. Lett.* **66**, 413 (1995).
- ⁵F. Lin, J. Zhao, T. Luo, M. Jian, Z. Wu, Y. Xie, Q. Quian, and H. Zeng, *J. Appl. Phys.* **74**, 2140 (1993).
- ⁶S. J. L. Ribeiro, R. E. O. Diniz, Y. Messaddeq, L. A. O. Nunes, and M. A. Aegerter, *Chem. Phys. Lett.* **220**, 214 (1994).
- ⁷C. X. Cardoso, Y. Messaddeq, L. A. O. Nunes, and M. A. Aegerter, *J. Non-Cryst. Solids* **161**, 177 (1993).
- ⁸J. Fernández, R. Bolda, and M. A. Arriandiago, *Opt. Mater.* **4**, 91 (1994).
- ⁹S. Kishimoto and K. Hirao, *J. Appl. Phys.* **80**, 1965 (1996).
- ¹⁰M. Dejneca, E. Snitzer, and R. E. Riman, *J. Lumin.* **65**, 227 (1995).
- ¹¹S. Tanabe, T. Hanada, M. Watanabe, T. Hayashi, and N. Soga, *J. Am. Ceram. Soc.* **78**, 2917 (1995).
- ¹²L. E. E. de Araújo, A. S. L. Gomes, C. B. de Araújo, Y. Messaddeq, A. Florez, and M. A. Aegerter, *Phys. Rev. B* **50**, 16 219 (1994).
- ¹³C. B. de Araújo, L. de S. Menezes, G. S. Maciel, L. H. Acioli, A. S. L. Gomes, Y. Messaddeq, A. Florez, and M. A. Aegerter, *Appl. Phys. Lett.* **68**, 602 (1996).
- ¹⁴G. S. Maciel, C. B. de Araújo, Y. Messaddeq, and M. A. Aegerter, *Phys. Rev. B* **55**, 6335 (1997).
- ¹⁵L. de S. Menezes, C. B. de Araújo, G. S. Maciel, Y. Messaddeq, and M. A. Aegerter, *Appl. Phys. Lett.* **70**, 683 (1997).
- ¹⁶N. Rakov, C. B. de Araújo, Y. Messaddeq, and M. A. Aegerter, *Appl. Phys. Lett.* **70**, 3084 (1997).
- ¹⁷J. Azkargota, I. Iparraguirre, R. Bolda, J. Fernández, E. Dénoue, and J. L. Adam, *IEEE J. Quantum Electron.* **QE-30**, 1862 (1994).
- ¹⁸G. S. Maciel, L. de S. Menezes, A. S. L. Gomes, Cid B. de Araújo, Y. Messaddeq, A. Florez, and M. A. Aegerter, *IEEE Photonics Technol. Lett.* **7**, 1474 (1995).
- ¹⁹R. P. de Melo, Jr., B. J. P. da Silva, E. L. Falcão-Filho, E. F. da Silva, Jr., D. V. Petrov, C. B. de Araújo, Y. Messaddeq, and M. A. Aegerter, *Appl. Phys. Lett.* **67**, 886 (1995).
- ²⁰Y. Maeda, *J. Appl. Phys.* **72**, 3835 (1992).
- ²¹Y. Maeda, S. Yamamoto, and M. Migitaka, *Appl. Phys. Lett.* **59**, 390 (1991).
- ²²Y. Maeda, S. Ikeda, and M. Migitaka, *Jpn. J. Appl. Phys., Part 2* **35**, L840 (1996).
- ²³Y. Maeda, *Appl. Opt.* **33**, 4077 (1994).
- ²⁴J. S. Chivian, W. E. Case, and D. D. Eden, *Appl. Phys. Lett.* **35**, 124 (1979).
- ²⁵F. Auzel and Y. H. Chen, *J. Lumin.* **65**, 45 (1995).
- ²⁶M. F. Joubert, S. Guy, and B. Jacquier, *Phys. Rev. B* **48**, 10 031 (1993).